ISBN: 978-3-95450-241-7 ISSN: 2673-5350 doi:10.18429/JACoW-IBIC2022-MOP23

RECENT LHC SR INTERFEROMETER SIMULATIONS AND EXPERIMENTAL RESULTS

D. Butti*,[1], E. Bravin, G. Trad, CERN, Geneva, Switzerland
S. Gibson, Royal Holloway, University of London, Egham, United Kingdom
[1]also at Royal Holloway, University of London, Egham, United Kingdom

Abstract

At the CERN Large Hadron Collider (LHC), among the different systems exploiting Synchrotron Radiation (SR) for beam diagnostics, interferometry is under study as a non-invasive technique for measuring absolute transverse beam sizes. Extensive numerical simulations, recently completed for characterising the spatial coherence of the LHC SR source, facilitated the optimisation of the LHC interferometer design and the existing prototype system tested in the past has been refurbished to include the new simulation findings. This contribution will describe the simulation specificity and then focus on the first measurements performed in a very tight schedule during the LHC Run 3 test run in October 2021. Such experiments allowed to obtain a first validation of the expected system performance at the injection energy of 450 GeV. A complete benchmark of the simulations will be carried out in 2022 as soon as the LHC will reach its top energy of 6.8 TeV.

INTRODUCTION

The transverse beam diagnostics at the Large Hadron Collider (LHC) is currently performed with two families of operational instruments [1]. Wire scanners (WS) provide an absolute size measurement but their usage is limited below a certain beam intensity due to damage to the wire caused by beam-wire interactions. A second instrument, the Beam Synchrotron Radiation Telescope (BSRT), exploits synchrotron radiation imaging for the continuous monitoring of the beam size. At present the BSRT cannot provide an absolute measurement and so a cross-calibration with the WS is required.

Synchrotron radiation interferometry is an optical technique, alternative to imaging, that can provide a non-invasive and absolute measurement of the transverse size of a luminous source [2]. This technique has been proposed for beam diagnostics [3] and it is currently exploited at the LHC to complement the operational instrumentation with a redundant and independent system [4].

The Beam Synchrotron Radiation Interferometer (BSRI) installed at the LHC is a classical Young's double slit interferometer. The visible synchrotron radiation (SR) emitted by the beam is sampled by two slits. The wavelets propagate through an optical system that produces the SR interferogram onto an intensified camera. The technique is based on a fundamental result of classical optics, the Van Citter and Zernike theorem (VCZ). This theorem states that the spatial coherence $|\gamma_{12}|$ of the points sampled by the slits coincides with the Fourier transform of the source transverse profile [5]. For Gaussian sources, the coherence as a function of the slit separation D is still a Gaussian

$$|\gamma_{12}| = \exp^{-\frac{D^2}{2\sigma_{coh}^2}} . \qquad (1)$$

The standard deviation $\sigma_{coh} = (\lambda L_0)/(2\pi\sigma)$ defines the coherence area of the radiation, where λ is the wavelength, L_0 the source distance and σ the source size.

Experimentally, the spatial coherence is measurable though the visibility of the radiation interferogram

$$V = \frac{2\sqrt{I_1 I_2}}{I_1 + I_2}|\gamma_{12}|, \qquad (2)$$

being I_1 and I_2 the total light transmitted through each aperture whose effect is to reduce the expected visibility if the slits are unevenly illuminated, i.e. $I_1 \neq I_2$.

The VCZ theorem strictly applies to thermal sources which consist of many point-like independent emitters radiating an isotropic wavefront. In case of non-thermal sources, such as SR radiated by relativistic beams, the theorem has to be validated on a case-by-case basis [6, 7].

In this paper, the unique features of the LHC SR source are presented and the results of the VCZ validation by means of SR simulations are discussed.

THE LHC SYNCHROTRON RADIATION SOURCE

The radiation source used for beam diagnostics at the LHC consists of two types of magnetic devices [8]. At injection energy, visible light is emitted by a superconducting undulator. As the beam energy increases, the undulator spectrum drifts towards the soft X-rays region. Above 2 TeV, the main source of visible light becomes the $D3_R$, a D3-type dipole located just downstream of the undulator. The undulator and the $D3_R$ are the main devices of the LHC SR source. A second D3-type dipole, the $D3_L$, contributes to the SR emitted at high beam energy. This dipole is located approximately 100 m upstream of the undulator, on the opposite side of the RF cavity section. After the source, the SR propagates for ~ 25 m inside the beam chamber until it is intercepted and extracted by an in-vacuum mirror that sends the light towards the BSRI slits. Figure 1 shows a layout of the source devices and the extraction system.

The contribution from the $D3_L$ has been recently detected with the SR interferometer [9]. The presence of this dipole is in fact negligible for the BSRT as it is far away from the

* daniele.butti@cern.ch

ISBN: 978-3-95450-241-7 ISSN: 2673-5350 doi:10.18429/JACoW-IBIC2022-MOP23

Table 1: Summary of the LHC Source Parameters Relevant to SR Interferometry, Comma Separated Values Refer to the Horizontal and Vertical Direction Respectively

Parameter	Injection	Flat-top	Unit
Device	Und	$D3_R$ (and $D3_L$)	-
Source dist. L_0	29.5	~ 26.7	m
Beta β	205, 287	200, 300	m
Beam size σ	1030, 1220	270, 330	µm
Coh. area σ_{coh}	2.5, 2.2	8.8, 7.2	mm
SR spot size	50, 50	10, 12	mm
Emittance ε_n	2.5		µm
Wavelength λ	400 - 560		nm

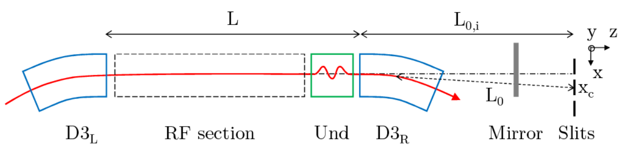

Figure 1: LHC synchrotron radiation source.

main $D3_R$ source and its light is completely out of focus at the final image. The interferometer does not focus light from any specific device. Although the $D3_R$ remains the main source of light at flat-top, the $D3_L$ light interferes with the $D3_R$ radiation and affects the wavefront arriving at the interferometer slits. SR from the two dipoles arrive at the slit plane with a phase delay $\Delta\varphi$ that can be written as

$$\Delta\varphi = \frac{2\pi}{\lambda}\left(\frac{L}{2\gamma^2} + \frac{r^2}{2L_{0,i}}\frac{L}{L+L_{0,i}}\right), \tag{3}$$

being γ the beam relativistic factor, L the $D3_L$ to $D3_R$ distance, L_0 the $D3_R$ to slit distance and $r^2 = x^2 + y^2$ the transverse radial coordinate at the slit plane. The first term of Eq. (3) represents the phase slippage between protons and light travelling between the dipoles. This gives a constant delay which does not create any modulation of the SR intensity distribution. The second term is purely geometrical and stems from the different curvatures of the two wavefronts at the slit plane. The r^2 factor gives rise to an interference pattern characterised by concentric fringes. Figure 2 shows an example of the synchrotron radiation arriving at the BSRI. The concentric rings created by the dipole interference are clearly visible in both the simulated and experimental intensity distributions.

SYNCHROTRON RADIATION SIMULATIONS

Extensive simulations have been carried out to investigate the applicability of the VCZ theorem to the case of the LHC SR source. The objective of the simulations is to verify that the model of Eqs. (1) and (2) allows to retrieve the beam size from the interferogram visibility within an accuracy of ± 2.5%. This tolerance is compatible with the ± 5% emittance uncertainty desired by the LHC operation.

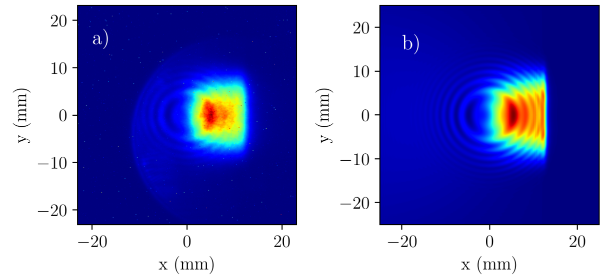

Figure 2: Experimental (a) and simulated (b) SR spatial distribution arriving at the slit plane at 6.8 TeV. The observation wavelength is 400 nm. The main lobe of the light is the SR emitted by the $D3_R$, modulated by the interference with the $D3_L$. The vertical cut at $x = 12$ mm is the edge of the extraction mirror. The circular cut in the background of (a) is created by the finite aperture of a filter wheel installed upstream of the observation screen.

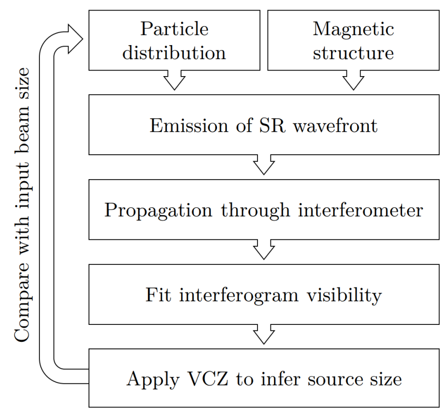

Figure 3: Simulation workflow.

Simulations are performed with a code based on Synchrotron Radiation Workshop (SRW), a standard tool for physical optics simulations of SR [10, 11]. The simulation strategy is outlined in Fig. 3. The code computes the wavefront emitted by a single particle sampled out of the beam distribution. The field is then propagated through the series of apertures and lenses of the interferometer to produce the single particle interferogram. The procedure is repeated and the beam interferogram is computed as the incoherent sum of the single particle ones. The resulting pattern is fitted to obtain the fringe visibility. The corresponding source size is computed using the VCZ relations and the result is compared to the one given as an input for the particle distribution.

Simulations confirm the VCZ theorem at injection energy along both the horizontal and vertical directions. This result is expected from the source parameters summarised in Table 1. The spatial distribution of the undulator radiation is much larger than its typical coherence area. This means that the light is almost uniform within its coherence area. The VCZ model is thus applicable in its canonical form.

ISBN: 978-3-95450-241-7 ISSN: 2673-5350 doi:10.18429/JACoW-IBIC2022-MOP23

The situation is more critical at 6.8 TeV. A typical flat-top beam size of 300 µm produces SR with a coherence area in the order of 8 mm. This value is comparable to the size of the available light spot. As a consequence, the emitted light cannot be considered as uniform within the coherence area, both because of its finite extent and the presence of the dipole interference effects. Another issue with the VCZ theorem at flat-top is the longitudinal position of the source, needed to define the source distance L_0. SR at flat-top is emitted along a beam trajectory that spans almost 4 m inside the D3$_R$ dipole so that a value for L_0 cannot be defined a priori. Both these issues hinder the applicability of the VCZ model in its standard formulation. Equation (1) provides nonetheless a compact and practical expression to retrieve the source size from the measured radiation coherence. The simulation campaign at flat-top aims to overcome these limitations. The goal is to search for configurations of the SR interferometer for which the VCZ equations provide an approximate estimation of the real source size, accurate within the required limits. For this purpose, the slit position and size have been optimised to minimise the effects of the nonuniform light distribution. On the other hand, the parameter L_0 has been defined as the distance between the slit centre x_c and the beam, measured along the tangent to the trajectory impinging on x_c, as illustrated in Fig. 1. For small beam deflections, this distance can be approximated as

$$L_0 \approx L_{0,i}\sqrt{1-\frac{2\rho x_c}{L_{0,i}^2}}, \tag{4}$$

being $\rho = 6013$ m the dipole bending radius and $L_{0,i} \approx 30$ m the longitudinal distance between the start of the magnet and the slit plane. It is important to stress that Eq. (4) does not identify an exact longitudinal position of the source at flat-top, whose longitudinal extension is an intrinsic feature of dipole radiation. The expression is a practical result that preserves the VCZ equations by just re-defining the source distance parameter.

An example of interferometry simulations at flat-top is reported, for the vertical direction, in Fig. 4. The coherence simulated with two point-like apertures (solid lines) is affected by the two dipole interference. By using properly extended slits (dashed lines), the dipole interference fringes are averaged and the oscillations of the coherence are damped. The coherence obtained with the optimised slit shape is in good agreement with the VCZ prediction, evaluated with the source distance definition of Eq. (4). In particular, any slit position with $x_c > 6$ mm features a discrepancy between simulations and analytical estimation within the required tolerance. This result proves that the VCZ formula is still valid to infer the beam size. The method relies only on the adoption of some specific slit configurations and a proper definition of the source distance. It is therefore suitable to be deployed in an operational instrument.

Similar considerations apply to the horizontal direction at flat-top. The main difference is the narrower region of slit positions where the VCZ formulas are applicable. This difference stems from the asymmetry of the dipole radiation in the horizontal direction, which leaves less margin for optimisation.

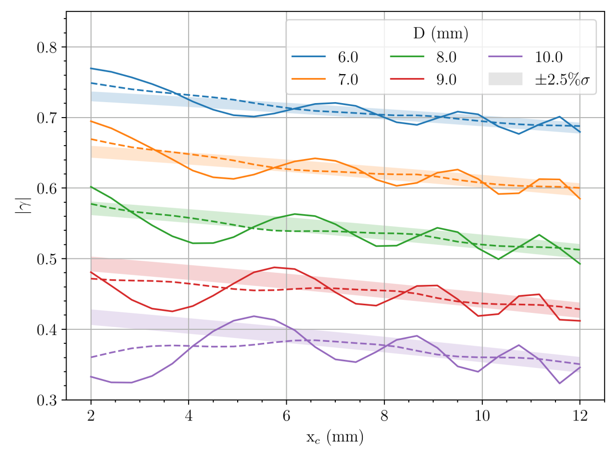

Figure 4: Simulations of the validity of the VCZ theorem along the vertical direction at 6.8 TeV and 560 nm observation wavelength. For several slit separations, the spatial coherence obtained by the simulated interferograms using Eq. (2) is plotted as a function of the horizontal slit centre. The results with standard square apertures of 0.5 mm × 0.5 mm (solid lines) are compared to an optimised configuration of rectangular slits of 0.5 mm × 4 mm (dashed lines). Color bands represent the VCZ prediction with a 2.5% tolerance.

HIGHLIGHTS FROM RUN 3 COMMISSIONING

The LHC SR interferometer has been refurbished for LHC Run 3 that started in spring 2022 and the upgraded setup is now being commissioned.

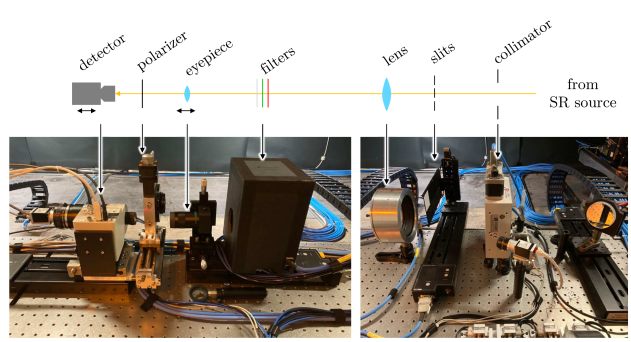

Figure 5: SR interferometer setup for LHC Run 3.

Figure 5 shows the hardware installed on the same table as the other LHC SR monitors. The whole setup is remotely controlled from a Python GUI which also provides a real-time processing of the acquired interferogram.

The instrument performance has been already validated by measuring nominal bunches at injection energy. Figure 6 reports an example of beam size monitoring. This measurement has been performed during two consecutive stable

ISBN: 978-3-95450-241-7   ISSN: 2673-5350   doi:10.18429/JACoW-IBIC2022-MOP23

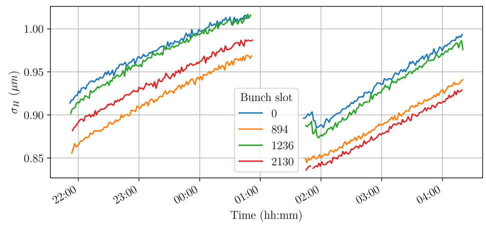

Figure 6: Horizontal beam size evolution during two stable beam fills with four bunches colliding at injection energy. The gap in the measurements corresponds to the time interval between the dump of the first fill and the injection of the second one.

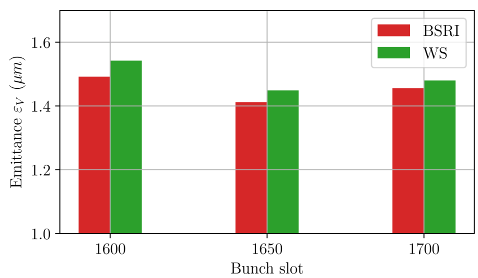

Figure 7: Comparison between the BSRI and WS measurements of the vertical emittance of three nominal bunches at injection energy.

beam fills at injection energy. The SR interferometer is able to resolve, with a precision better than 2%, the different sizes of the four circulating bunches. The beam size growth induced by the collisions is clearly visible throughout each fill.

The absolute measurement at injection energy is also compatible with the reference values provided by the wire scanner. A comparison of the vertical emittance measurement for three bunches is displayed in Fig. 7. The emittance measured by the two instruments agrees within 3%. The BSRI performance along the horizontal direction is similar, thanks to the axial symmetry of the undulator radiation.

Some discrepancies are present at 6.8 TeV. Although a relative measurement is still achievable, the absolute value of the emittance is systematically higher than the reference one provided by the WS. This means that the acquired interferograms have a lower visibility than the expected one. Investigations are ongoing to identify the origin of this discrepancy. Some common causes of visibility loss, for example mechanical vibrations in the setup, have been already excluded as possible causes. Tests are currently ongoing to identify whether some specific component of the hardware is responsible for the loss of visibility. In parallel to the investigations on the setup, data analysis aims at searching for some general correction that would allow to compensate for this effect in a self-consistent way.

CONCLUSION

The status of SR interferometry at the LHC has been presented in this contribution. Despite the challenging scenario given by the LHC SR source, simulations show that the technique is theoretically exploitable for absolute beam size measurements. The VCZ theorem can be used to infer the beam size from the measured interferogram visibility. At injection energy, the theorem is valid in its canonical form. The complexity of the SR source at flat-top affects the VCZ model. Simulations allow to optimise the slit configurations and provide a specific definition of the source distance so that the analytical result offered by the VCZ theorem can still be used to retrieve the beam size.

The benchmarking of such simulations is ongoing. Preliminary results confirmed the scenario at injection energy while some discrepancies are still present at 6.8 TeV, where the measured visibility is systematically lower than the expected one. Investigations are ongoing to identify the sources of the visibility loss or to find a self-consistent way to compensate for it.

REFERENCES

[1] G. Trad *et al.*, “Status of the beam instrumentation at the LHC”, in *Proc. 7th Evian Workshop on LHC beam operation*, Evian Les Bains, France, Dec. 2016, pp.185–192.

[2] J. Goodman, *Introduction to Fourier Optics, 4th Edition*, NY, USA: W. H. Freeman, 2017.

[3] T. Mitsuhashi, “Beam profile and size measurement by SR interferometers”, in *Beam measurement*, World Scientific, 1999, pp. 399–427. doi:10.1142/9789812818003_0018

[4] G. Trad, “Development and optimisation of the sps and lhc beam diagnostics based on synchrotron radiation monitors”, Ph.D. thesis, Université Grenoble Alpes, Saint-Martin-d’Hères, France, 2015.

[5] F. Zernike, “The concept of degree of coherence and its application to optical problems”, *Physica*, vol. 5, pp. 785–795, 1938. doi:10.1016/S0031-8914(38)80203-2

[6] G. Geloni, E. Saldin, E. Schneidmiller, and M. Yurkov, “Transverse coherence properties of x-ray beams in thirdgeneration synchrotron radiation sources”, *Nucl. Instrum. Methods Phys. Res., Sect. A*, vol. 588, pp. 463–493, 2008. doi:10.1016/j.nima.2008.01.089

[7] Y. Takayama and S. Kamada, “Spatial coherence of bending magnet radiation and application limit of the van Cittert–Zernike theorem”, *Phys. Rev. E*, vol. 59, p. 7128, 1999. doi:10.1103/PhysRevE.59.7128

[8] L. Ponce, R. Jung, and F. Méot, “LHC proton beam diagnostics using synchrotron radiation”, CERN, Geneva, Switzerland, Rep. CERN-2004-007, 2004. doi:10.5170/CERN-2004-007

[9] D. Butti, “Synchrotron radiation interferometry for beam size measurement at the Large Hadron Collider”, M.S. thesis, Politecnico di Milano, Milan, Italy, 2019.

[10] O. Chubar, http://github.com/ochubar/SRW

[11] O. Chubar and P. Elleaume, “Accurate and efficient computation of synchrotron radiation in the near field region”, in *Proc. EPAC’98*, Stockholm, Sweden, Jun. 1998, pp. 1177–1179.